Nature of the ferromagnetism induced by nonmagnetic substitutions on the Ru site of $CaRuO_3$

V. Hardy, B. Raveau, R. Retoux, N. Barrier, and A. Maignan

Laboratoire CRISMAT, Unité Mixte de Recherches 6508, Institut des Sciences de la Matière et du Rayonnement, Université de Caen, 6, Boulevard du Maréchal Juin, 14050 Caen Cedex, France

In spite of many efforts, the magnetic ground state of $CaRuO_3$ remains enigmatic to date and is still the subject of intense controversy. Among the peculiarities of this ruthenate is the puzzling fact that small levels of substitution on the magnetic Ru^{4+} sublattice by nonmagnetic cations were found to induce the development of a ferromagnetic transition. The present paper addresses this issue by combining magnetization, resistivity, and heat capacity measurements in $CaRu_{1-x}M_xO_3$ for $0 \leq x < 1$ and M = Ti, Zr, Ga, and Al. It is suggested that this substitution-induced ferromagnetism is basically heterogeneous and itinerant in nature.

I. INTRODUCTION

The ruthenates belonging to the Ruddlesden-Popper series $(Sr,Ca)_{n+1}Ru_nO_{3n+1}$ have been attracting strong interest in the past few years owing to their intriguing physical properties, such as the unconventional superconductivity found in the n=1 term, Sr_2RuO_4.[1] Another issue being still the subject of intense activity is the comparison between the n=∞ terms, $SrRuO_3$ and $CaRuO_3$.[2–7] These two compounds present the same perovskite structure with orthorhombic distortion, the same Ru^{4+} valence state, and they both show metalliclike resistivity. On the other hand, their magnetic properties are totally different: While $SrRuO_3$ is an itinerant ferromagnet with $T_C \sim 160$–165 K,[8,9] its counterpart $CaRuO_3$ does not show long-range ordering down to 30 mK,[10] and its magnetic ground state is still enigmatic. It must be noted that the only structural difference between the Sr- and Ca-based compounds is about the degree of orthorhombic distortion, which is a bit larger in the latter due to the smaller size of Ca^{2+} compared to Sr^{2+}. In the literature, a lot of suggestions have been made about the nature of magnetism in $CaRuO_3$, including localized antiferromagnetism,[9] spin-glasslike state,[11] and exchange-enhanced paramagnetism[6] or nearly itinerant ferromagnetism.[5,7] We note that this controversy on ruthenates is made delicate by the difficulty to predict *a priori* which approximation, strongly correlated or band structure based, is best suited to the magnetism of oxides with such $4d$ elements.[4] Concerning $CaRuO_3$, the only point which is widely accepted so far is the fact that this compound would be *on the verge of a ferromagnetic instability*.[2,4,12]

Peculiar effects of B site substitutions in $CaRuO_3$ made the case of this compound still more intriguing. It was shown that small levels of substitution by certain elements can generate various magnetic states in $CaRu_{1-x}M_xO_3$, such as ferromagnetism[13–16] with M = Ti, Fe, Ni, and Mn, or weaker ordering (maybe related to spin-glass behavior)[2,17,18] with M = Cu, Sn, and Rh. Among these results, one of the most striking is the case of the substitutions by Ti for Ru.[13,16] It was found that substitution with this nonmagnetic, isovalent cation (Ti^{4+} being $3d^0$) leads to ferromagnetic ordering, a result which may appear paradoxical for a random magnetic dilution. It has been concluded that $CaRuO_3$ is poised at a critical point between ferromagnetism and paramagnetism, a balance tipped in favor of the former by small amounts of disorder.[13] However, the nature of this link between disorder and ferromagnetism remains to be specified. Furthermore, we underline that experimental features of the Ti-induced ferromagnetism are still a matter for debate. For instance, the Curie temperature T_C was reported to be 55 K by He *et al.*,[13] whereas Felner *et al.*[16] found 34 K. The influence of the substitution level is another open question. He *et al.* emphasized the striking fact that ferromagnetism can be induced by Ti content as low as 2%, but it is also remarkable that the same T_C is still observed for substitution contents as large as 80%.[13] In other respects, one may wonder about a possible specificity of Ti, since a different effect was found when substituting by Sn,[2] while the latter element is supposed to yield nonmagnetic Sn^{4+} just like Ti^{4+}.

The present study was aimed to carry on the analysis of such nonmagnetic substitutions on the B site of $CaRuO_3$. Our work was focussed on the series $CaRu_{1-x}Ti_xO_3$, with x going from 0 to 1 by 0.1 steps. Comparisons were made with substitutions by other nonmagnetic cations, such as the tetravalent Zr or the trivalent Ga and Al, considering x=0.2. The evolution of the physical properties was investigated by magnetization, resistivity, and specific heat measurements.

II. EXPERIMENTAL DETAILS

Polycrystalline samples were synthesized from intimate mixtures of oxides, i.e. CaO, RuO_2, and MO_2 (for M = Ti, Zr, Sn) or M_2O_3 (for M = Al, Ga), first heated at 800 °C for 12 h, and then sintered at 1300 °C for 13 h. The samples were then slowly cooled down to 800 °C before being quenched to room temperature.

X-ray powder diffraction patterns were recorded on a PANalytical X'pert MPD Pro diffractometer, equipped with a X'Celerator detector. The data were recorded at room temperature, over the $15°$–$140°(2\theta)$ range with ~$0.017°$ increments in 2θ. In most cases (M = Ti, Al, and Ga), the patterns attested of the purity of the so obtained perovskites. An example of such diffraction patterns is shown in the main panel of Fig. 1. Special attention was paid to the case of M = Ti, for which different x values were investigated. Rietveld
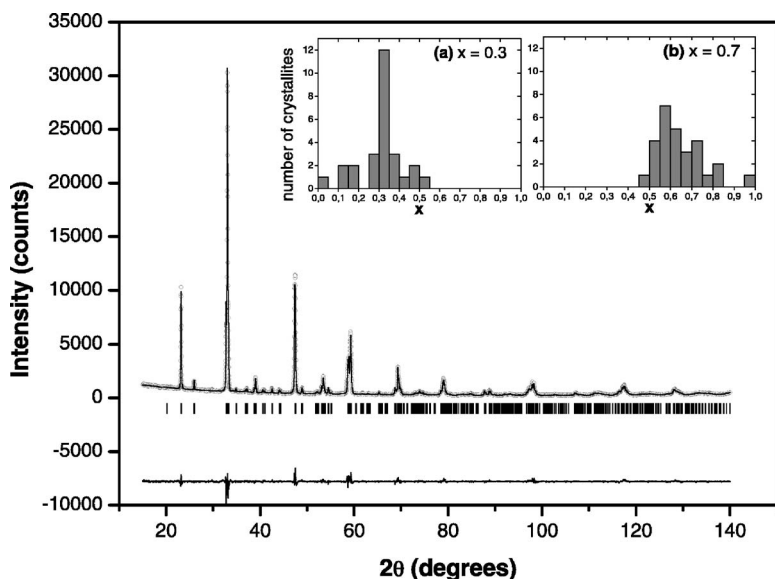
FIG. 1. Rietveld refinement of the x-ray powder diffraction pattern of $CaRu_{0.3}Ti_{0.7}O_3$. The observed pattern corresponds to the dots; the solid line is the calculated pattern; the difference profile is shown at the bottom. The small ticks below the patterns are the positions of the Bragg reflections in the orthorhombic *Pnma* space group. The insets display histograms corresponding to EDS analyses of crystallites from the nominal compositions (a) $CaRu_{0.7}Ti_{0.3}O_3$ and (b) $CaRu_{0.3}Ti_{0.7}O_3$.

refinements were carried out using the program Fullprof[19] in the orthorhombic *Pnma* space group. For instance, in the case of $x=0.7$ shown in Fig. 1, the refined unit-cell parameters are $a=0.54589(2)$ nm, $b=0.76542(3)$ nm, and $c=0.53849(2)$ nm. The conventional reliability factors for the pattern are $R_p=5.62\%$, $R_{wp}=7.66\%$, $R_{exp}=3.77\%$, with $\chi^2=3.54$, as well as $R_F=3.99\%$ for the structure. As a whole, our study of $M=$Ti confirmed the existence of a pure solid solution in the system $CaRu_{1-x}Ti_xO_3$ for x ranging from 0 to 1. It must be specified, however, that parasitic phases were detected in a few cases, without showing any relationship with the x value (most probably, the lesser sample purity observed in some samples can be ascribed to slight, uncontrolled differences in the synthesis conditions). X-ray analysis revealed that the main foreign phase has the structure of $Ca_3Ru_2O_7$, and it represents a small fraction which—even in the worst case—remains lower than 8 wt. %. It must also be noted that $Ca_3Ru_2O_7$ was reported to exhibit an antiferromagnetic transition at $T\sim 56$ K,[20] i.e., a behavior completely different from the magnetic features that will be shown to occur in these $CaRu_{1-x}Ti_xO_3$ samples (see next section). In the case of $CaRu_{1-x}Sn_xO_3$, we did not succeed in preparing a compound with a purity good enough to allow a reliable analysis of the physical properties (even qualitative). In the case of the system $CaRu_{1-x}Zr_xO_3$, a pure phase could not be obtained, but the greatest part of our samples were found to have a perovskite structure $Ca(Ru,Zr)O_3$.

For some selected compositions, numerous crystallites were characterized using electron diffraction (ED) in order to investigate the homogeneity in composition of our samples. To do so, ceramic bars were crushed in *n*-butanol, and crystallites present in the suspension were deposited onto a holey carbon film supported by a nickel grid. The ED was performed on JEOL 200CX and JEOL 2010 electron microscopes (tilt ±60°) equipped with EDS analyzers and tilting rotating sample holders. Such EDS studies were mainly carried out in the $CaRu_{1-x}Ti_xO_3$ system. In all cases, the cationic compositions of most of the crystallites were found to be consistent with the nominal one. More precisely, we obtained distributions of the experimental x values that show a

Gaussian-type shape centered close to the expected x value, along with with a few grains having clearly shifted compositions. For all investigated x values (i.e., 0.2, 0.3, 0.7, and 0.8), it can be noted that: (i) the proportion of grains having strongly shifted compositions is very small (typically 5%); (ii) the center of the distribution is in reasonable agreement with the nominal value (the largest shift was found with the nominal $x=0.7$ for which the experimental distribution is centered at ~ 0.62); (iii) the half-width at half-maximum of the distribution is lower than $\Delta x\simeq 0.15$, in all cases. Two examples of histograms derived from these EDS analysis are displayed in Fig. 1.

EDS analysis was also performed in a sample of nominal composition "$CaRu_{0.8}Zr_{0.2}O_3$," which turns out to yield a remarkable ferromagnetic transition (see next section). Although this compound is not pure, the x-ray study showed that a peroskite phase is predominant. Our goal was to make sure that Zr actually enters into the $CaRuO_3$ matrix. The EDS analysis demonstrated that, within the accuracy of the technique, about 80% of the grains exhibit compositions compatible with the expected one, i.e., close to "$CaRu_{0.8}Zr_{0.2}$." Since—to the best of our knowledge—there is no well-known ferromagnetic Ca-based oxides containing Ru and/or Zr, we consider that the peculiar ferromagnetism developing in this sample can safely be ascribed the perovskite $CaRu_{0.8}Zr_{0.2}O_3$.

Both specific heat and magnetization measurements were carried out in a Physical Properties Measurement System (Quantum Design), with magnetic fields up to 9 T and temperatures down to 2 K. Specific heat measurements were derived from a relaxation method, while magnetization measurements were performed with an extraction technique. Zero-field resistivity measurements were collected using the standard four-probes technique, at temperatures between 2 and 380 K.

III. RESULTS

Figure 2(a) shows two curves of dc susceptibility ($\chi_{dc}=M/\mu_0 H$) as a function of the temperature, for $x=0.2$. Both
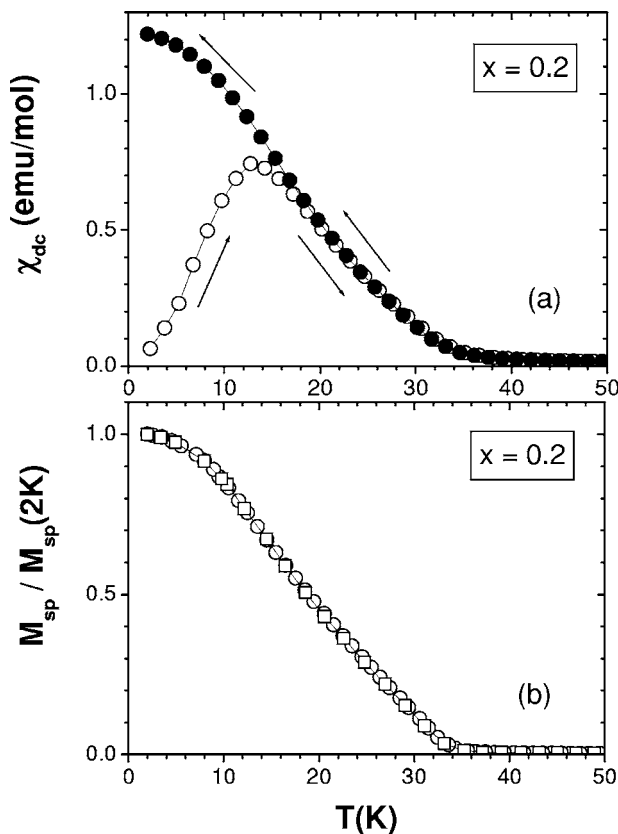
FIG. 2. Magnetic investigations of the ferromagnetic transition in $CaRu_{1-x}Ti_xO_3$ for $x=0.2$. (a) dc susceptibility recorded in 0.05 T upon warming after zero-field-cooling (open circles), and upon cooling in magnetic field (filled circles). The arrows indicate the direction of the temperature variation. (b) Normalized spontaneous magnetization recorded upon cooling in the remanent field of the coil ($\sim$5 Oe). The squares and circles correspond to two samples.

curves were collected in a magnetic field of 0.05 T, one of them after zero-field cooling (ZFC curve), while the other was recorded in the field-cooled cooling mode (FCC curve). On the ZFC curve, χ_{dc} is found to start from very low values. Upon warming, χ_{dc} first increases with T, then exhibits a peak, and finally decreases until merging onto the paramagnetic susceptibility around 35 K. The FCC and ZFC curves are superimposed on each other within the high-T range, but they diverge below approximately the temperature of the ZFC peak, since the FCC curve increases continuously as T is decreased. This set of features is typical of the ferromagnetic response of a material having its Curie temperature (T_C) close to 35 K and coercive fields (at the lowest T) being larger than the applied field. In such a case, the peaked shape of the ZFC curve can simply be ascribed to the thermally assisted magnetization process of a *hard* structure of disoriented ferromagnetic domains.

The crossover visible around 35 K in Fig. 2(a) was found to broaden as the field is increased. It is known that the best characterizations of a ferromagnetic transition require magnetic field values as low as possible. Figure 2(b) shows curves of spontaneous magnetization (M_{sp}) that were recorded upon cooling in nominally "zero-field," i.e., actually the remanent field of the coil, which was estimated to be
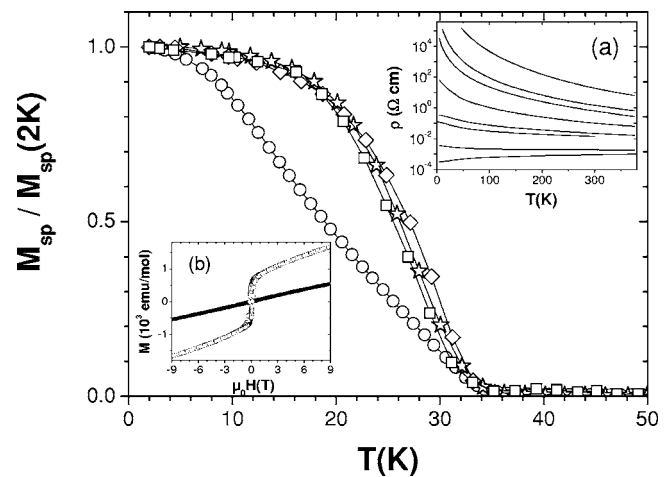

FIG. 3. Main panel: Normalized spontaneous magnetization of $CaRu_{1-x}Ti_xO_3$ for some x values: 0.2 (circles); 0.4 (stars); 0.6 (diamonds); 0.8 (squares). Inset (a) Evolution with x of the resistivity curves in zero-field. From bottom to top, the x values are 0/0.1/0.2/0.3/0.4/0.5/0.6/0.8. Inset (b) Full hysteresis loops at 5 K for the unsubstituted $CaRuO_3$ (filled circles) and for $CaRu_{1-x}Ti_xO_3$ with $x=0.2$ (open circles).

about 5 Oe in our case. Since this field can slightly vary from run to run, we present curves that were normalized by the value obtained at the lowest temperature (2 K). On these curves, one observes a well defined increase taking place at 34 K. It is worth noticing that this kink is more pronounced than in the upper panel. Furthermore, the close agreement found between two independent measurements shows the good reproducibility of this feature. Therefore, in the present study, we have used such spontaneous magnetization curves to characterize the T_C of the compounds. In the case of $x=0.2$, one obtains $T_C=34$ K. It can be noticed that the thermoremanent curve recorded on this sample led to the same value of T_C.

The main panel of Fig. 3 shows normalized $M_{sp}(T)$ curves for various x values ranging from 0.2 to 0.8. It is striking that all of them exhibit the same T_C. Actually, this $T_C=34$ K was found for all the x values, from 0.1 up to 0.9 (all the curves are not shown for sake of clarity). Besides, it can be noted that the curves corresponding to $x<0.3$ (e.g., $x=0.2$ in Fig. 3) were found to be broader than the others.

Inset (a) shows the evolution with x of the resistivity curves in zero-field $[\rho(T)]$. The curve for $x=0$ is well in line with the literature,[3] showing $\rho(300 \text{ K})\sim10^{-3}$ Ω cm and a metallic behavior. It must also be noted that the continuous and fast upward shift of $\rho(T)$ with x is in agreement with the previous study of He *et al.*[13] Inset (b) shows an example of the $M(H)$ curve at low-T in a substituted compound ($x=0.2$), along with the corresponding curve of the unsubstituted compound. While the curve of $CaRuO_3$ is essentially linear and without noticeable hysteresis, the curve of $x=0.2$ shows a characteristic ferromagneticlike shape. In agreement with the previous studies,[13,16] the coercive fields at such low-T are about 0.1 T. It is also of importance to underline that these $M(H)$ curves do not show saturation, whatever the x value.
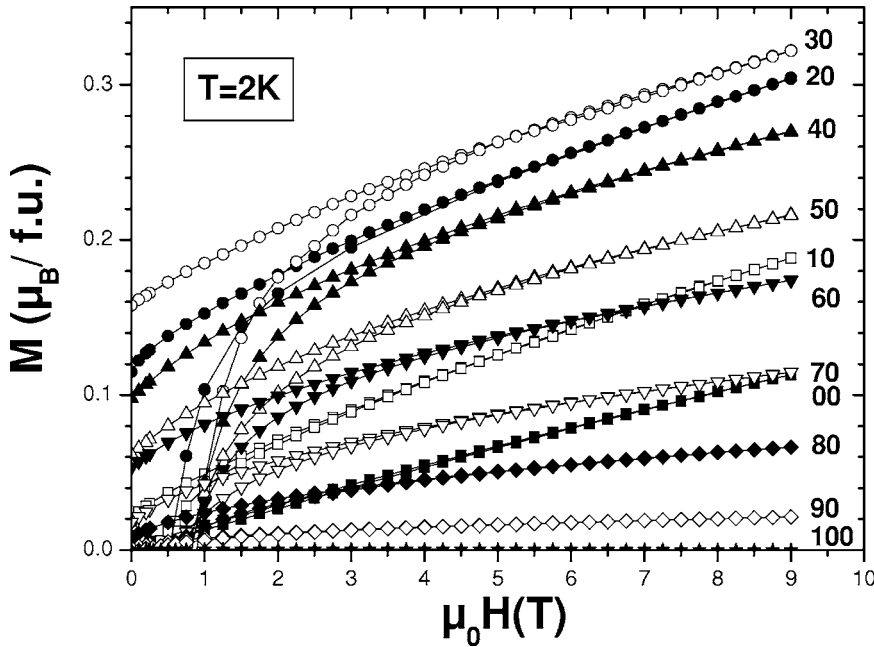
FIG. 4. Half hysteresis loops recorded at 2 K in CaRu$_{1-x}$Ti$_x$O$_3$, for x varying from 0 to 1 by 0.1 steps (the labels on the right are the Ti percentages on the B site, i.e., 100 x).

Figure 4 shows the half-loops recorded at $T=2$ K for all the x values (these data correspond to the first quadrant portion of the complete loops, i.e., omitting the virgin magnetization curves). Except for $x=0$ and $x=1$, all the curves exhibit the rounding characteristic of ferromagnetism (including $x=0.9$, even though it is not well visible at this scale). The location of the high-field parts of the curves first shift upward as x increases up to 0.3, and then go downward. It must be pointed out that the maximum still takes place at $x=0.3$, even if one normalizes the magnetization curves to the content of magnetic ions (i.e., M in μ_B/Ru).

For titanium on the B site of oxides with perovskite structure, one expects a valence state Ti^{4+}, but the possibility of Ti^{3+} cannot be totally ruled out. In such a case, the Ru should take a mixed valency Ru^{4+}/Ru^{5+} which might be at the origin of ferromagnetism. To investigate the impact of such a mixed valency, we compared the present behavior observed with Ti with those observed with trivalent, nonmagnetic ions such as Ga^{3+} and Al^{3+}. Figure 5(a) shows the $M(H)$ curve measured at 2 K in CaRu$_{0.8}$Ga$_{0.2}$O$_3$. The curve clearly has a rounded shape and one observes a large increase in magnetization with respect to the unsubstituted compound, but the key point is that there is no significant hysteresis. The same features were found with Al^{3+}. This absence of hysteresis is not consistent with the ferromagnetic properties induced by substitutions in CaRuO$_3$.[14] Moreover, the $M_{sp}(T)$ curves in Ga or Al substituted compounds did not show an abrupt increase at any temperature. Therefore, these results found with Ga and Al tend to discard the relevancy of a Ru^{4+}/Ru^{5+} valency (induced by the presence of Ti^{3+}) to the effect of Ti substitution in the present study.

Still with the aim of investigating possible peculiarities of Ti, we carried out substitutions with Zr, which is expected to yield tetravalent, nonmagnetic Zr^{4+}, exactly like Ti. Figure 5(a) shows the $M(H)$ curve measured at 2 K in a nominal CaRu$_{0.8}$Zr$_{0.2}$O$_3$ compound. Even though the bad purity of this compound hinders quantitative analysis, it must be em-

phasized that the shape of the curve is strikingly similar to that of the Ti-based counterpart. In both cases, one observes a pronounced rounding and a significant hysteresis on the $M(H)$ curves. Furthermore, Fig. 5(b) shows a remarkable agreement between the normalized $M_{sp}(T)$ curves of Ti and Zr for $x=0.2$. In conclusion, one can reasonably state that Zr substitution in CaRuO$_3$ also induces ferromagnetism with T_C close to 35 K, i.e., a behavior very close to that found with Ti.

In the absence of saturation on the $M(H)$ curves, the remanent magnetization M_{rem} is a relevant quantity to evaluate the strength of the ferromagnetism. Figure 6 shows the evolution of the ferromagnetic response with the Ti content, i.e., $M_{rem}(x)$. This curve first exhibits a pronounced upward curvature at low x, then a quite sharp peak around 0.3, and finally it decreases slowly, vanishing only around $x=0.9$.[21]

The possible origins of this substitution-induced ferromagnetism cannot be discussed without addressing first the question of the type of magnetism one is dealing with. Indeed, the present situation—involving a disordered lattice of 4d magnetic centers—can be expected to yield either localized or itinerant magnetism.[4] From an experimental point of view, the distinction between these two types of ferromagnetism is most often based on the comparison between the spontaneous ($T \ll T_C$) and the effective ($T \gg T_C$) magnetic moments.[22,23]

The main panel of Fig. 7 shows the reciprocal susceptibility versus temperature in the case of $x=0.3$. One observes a remarkable linear regime which holds over a broad temperature range. The same features were found with all the x values for which we recorded this type of data ($0.1 \leq x \leq 0.5$). It must be emphasized that the mere observation of such a Curie-Weiss (CW) behavior does not help to distinguish between the two types of ferromagnetism since this feature turns out to be expected in both cases. Indeed, very nice "CW-like" behaviors are theoretically predicted and experimentally observed in the case of some itinerant
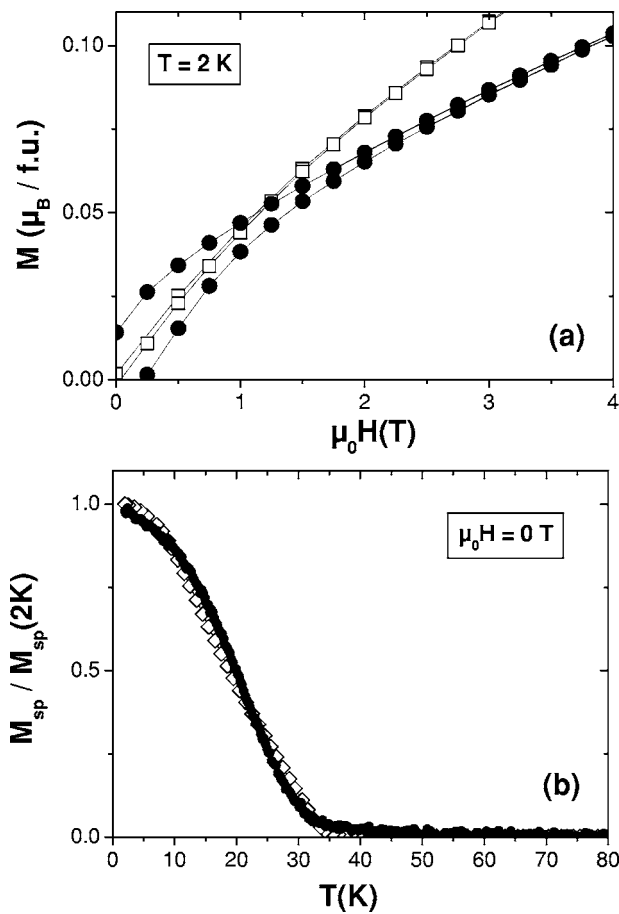
FIG. 5. Top panel: Half-loops recorded at 2 K in $CaRu_{0.8}M_{0.2}O_3$ for M=Zr (filled circles) and M=Ga (open squares). Bottom panel: Normalized spontaneous magnetization in $CaRu_{0.8}M_{0.2}O_3$ for M=Zr (filled circles) and M=Ti (open diamonds).

ferromagnets.[22,24] With CW plots, the extrapolation to $1/\chi$ =0 defines a characteristic temperature θ_{CW}. Within the framework of localized magnetism, the sign of θ_{CW} directly reflects the nature of the interactions, e.g., it must be positive in the case of ferromagnetic coupling. In contrast, for

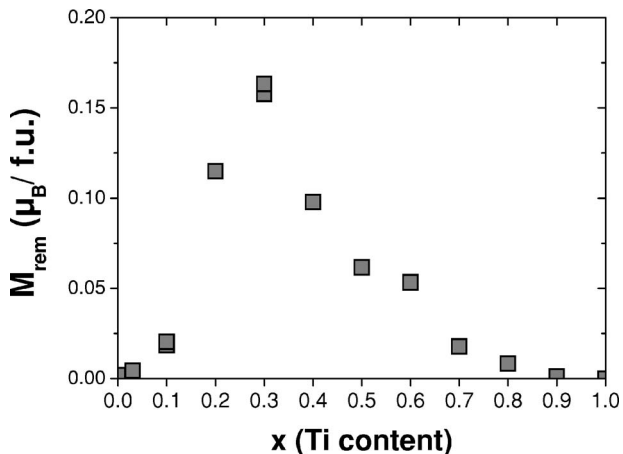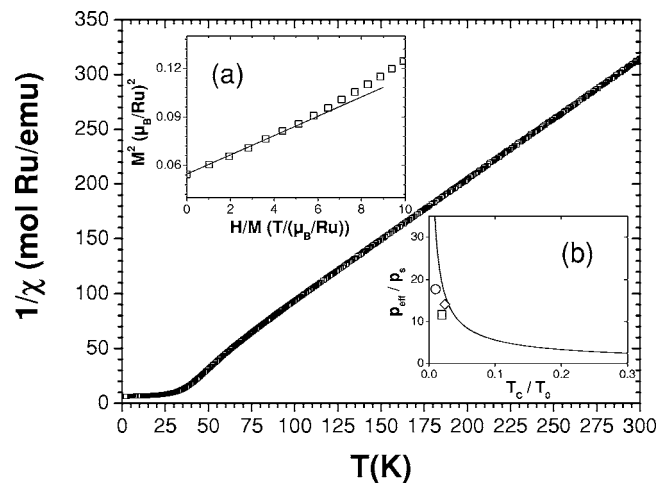FIG. 6. Remanent magnetization at 2 K in $CaRu_{1-x}Ti_xO_3$ as a function of x.

FIG. 7. Main panel: Temperature dependence of the reciprocal susceptibility of $CaRu_{1-x}Ti_xO_3$ for x=0.3. Inset (a) shows the Arrott plot for x=0.3 and T=2 K. Inset (b) is the generalized Rhodes-Wohlfarth plot with the data points of $CaRu_{0.7}Ti_{0.3}O_3$ (square), $CaRu_{0.8}Ti_{0.2}O_3$ (circle), and that of Sr_2CaRuO_7 (diamond) from Ref. 27. The solid line is the theoretical curve predicted by Taka-hashi for weakly itinerant ferromagnets (Ref. 23).

itinerant ferromagnetism, the θ_{CW} can be either <0 or >0, and it is actually found to be negative in a lot of cases.[24] In the present study, we have found a large negative value $\theta_{CW} \simeq -65$ K for x=0.1, a less negative value $\theta_{CW} \simeq -5$ K for x=0.2, and positive values for x within the range 0.3–0.5, as shown in Fig. 7 for x=0.3. These values still increase with x, from $\theta_{CW}(x$=0.3$) \simeq +10$ K to $\theta_{CW}(x$=0.5$) \simeq +20$ K. It can be noted that these results differ from the previous study, where negative θ_{CW} were found for all x values.[13] At first glance, the positive θ_{CW} found for the largest x values can be regarded as being consistent with the localized picture. Nevertheless, the simple fact that $\theta_{CW} \ll 0$ for x=0.1 casts doubt on this assumption, because one should expect the FM to be of same nature for all x values since they all exhibit the same T_C.

A well known means to estimate the degree of itinerancy is based on the Rhodes-Wohlfarth plot,[25] showing p_C/p_S vs T_C, where p_S is the spontaneous moment per magnetic ion, while p_C derives from the effective moment through the relation $p_{eff}^2 = p_C(p_C+2)$. In the case of pure localized magnetism, p_C/p_S=1, while in the opposite weakly FM limit, this ratio is supposed to increase as T_C decreases. It was experimentally found that all weakly itinerant ferromagnets give values of p_C/p_S lying onto—or slightly below—a limit curve that diverges as $T_C \rightarrow 0$.[22] Analysis of the CW regime of Fig. 7 leads to p_{eff}=2.69 μ_B/Ru, which is close to the theoretical value of 2.83 μ_B/Ru expected for Ru^{4+} (S=1 with g=2). From the experimental p_{eff}, one deduces p_C=1.87 μ_B/Ru. The spontaneous moment p_S can be derived from Arrott plots at $T \ll T_C$, by considering the intercept of the linear regime with the vertical axis. Inset (a) of Fig. 7 displays such a plot for T=2 K, from which one obtains p_S=0.23 μ_B/Ru, a value which simply corresponds to the remanent magnetization per Ru ion in the present case. One finally obtains $p_C/p_S \simeq 7.5$, which is substantially larger than 1, suggesting a marked

itinerant character. Associating this value with $T_C = 34$ K yields a point on the Rhodes-Wohlfarth plot which is located close to the experimental limit curve for weakly itinerant ferromagnets (WIF).[22] It can be noted that this point lies near those obtained for materials known as prototypical WIF such as Pd-Rh-Fe or Pd-Co alloys.[22]

More recently, Takahashi has proposed a generalized Rhodes-Wohlfarth plot on the basis of self-consistent renormalization theory of spin fluctuations.[23] Within this approach, all WIF are supposed to lie onto a universal curve in a p_{eff}/p_S vs T_C/T_0 plot, where T_0 is a characteristic temperature reflecting the energy width of the spin-fluctuations spectrum. The derivation of T_0 first requires the estimate of the fourth-order coefficient ($\overline{F_1}$) of the magnetic free energy. From a Arrott plot at $T \ll T_C$ like that of inset (a) of Fig. 7, $\overline{F_1}$ can be derived from the slope α of the linear regime at low fields: $\overline{F_1} \simeq 1.075 \times 10^{-3}/\alpha$, where $\overline{F_1}$ is in K and α in μ_B^3/T. Then, T_C/T_0 is calculated using the formula

$$\left(\frac{T_C}{T_0}\right)^{5/6} = \frac{p_S^2}{8\sqrt{15}\gamma}\left(\frac{\overline{F_1}}{T_C}\right)^{1/2}, \quad (1)$$

where $\gamma \simeq 0.3353$. Following this procedure with $CaRu_{0.7}Ti_{0.3}O_3$, we found a point of coordinates $T_C/T_0 \simeq 0.021$ and $p_{eff}/p_S \simeq 11.7$, which is reported in inset (b) of Fig. 7. This figure also includes the result of the same analysis performed on $CaRu_{0.8}Ti_{0.2}O_3$, as well as the theoretical curve of the model. Comparing with all the data gathered by Takahashi,[23] one observes that the points corresponding to our Ti-substituted ruthenates are as close to the universal curve as those of typical weakly itinerant ferromagnets (WIF), like Sc_3In or $NiPt$. In this generalized Rhodes-Wohlfarth plot, it can also be noted that our data lie close to that of the ruthenate $Sr_2CaRu_2O_7$, which was recently claimed to be a WIF.[27]

Still with the aim to specify the nature of ferromagnetism in $CaRu_{1-x}Ti_xO_3$ compounds, heat capacity measurements have been carried out. Figure 8 shows the temperature dependence of the heat capacity of $CaRu_{0.7}Ti_{0.3}O_3$ in zero-field, along with that of $CaZrO_3$. The latter compound is a nonmagnetic, isostructural compound which can be used to estimate the phonon contribution to the heat capacity. First of all, it must be pointed out that there is no peak at $T \sim T_C$ on the $C(T)$ curve of $CaRu_{0.7}Ti_{0.3}O_3$. A closer look at the shape of the curve, however, suggests the presence of an anomaly in the temperature dependence. This is more clearly revealed in a C/T vs T^2 plot which shows a smooth bump developing at temperatures lower than T_C (see inset of Fig. 8). To go further, we tried to extract the magneto-electronic contribution (C_{ME}) by subtracting the phonon contribution (C_{ph}). The latter term can itself be obtained from the heat capacity of the isostructural, nonmagnetic compound (C_{ref}), after suitable mass correction. Using the method detailed by Bouvier *et al.*[26]—which is valid within the low-T range under consideration—the phonon contribution in $CaRu_{0.7}Ti_{0.3}O_3$ was estimated by calculating $C_{ph}(T) = C_{ref}(T/r)$, with $r = 1.0158$. The resulting $C_{ME}(T)$ curve shown in Fig. 9 clearly exhibits a rounded bump centered at a temperature lower than T_C. Moreover, one can notice the presence of a
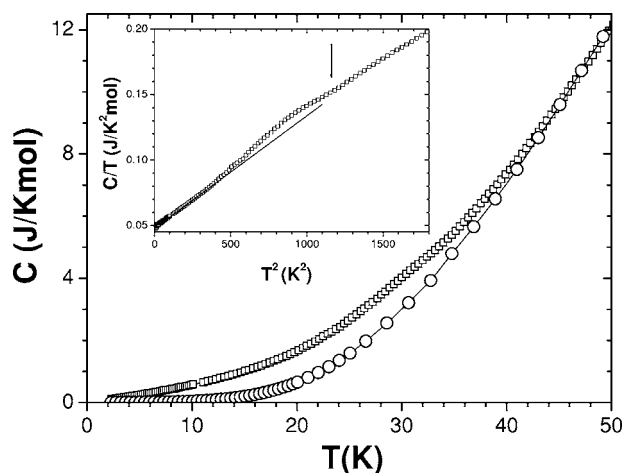

FIG. 8. Main panel: Temperature dependence of the heat capacity of $CaRu_{0.7}Ti_{0.3}O_3$ (squares) and of the nonmagnetic, isostructural compound $CaZrO_3$ (circles). The inset show the data of $CaRu_{0.7}Ti_{0.3}O_3$ in a C/T vs T^2 plot. The arrow indicates the T_C derived from magnetization data. The solid line is an extrapolation of the low-T linear regime.

kink located at T_C, on the decreasing part of the curve. The data that was recorded on a second sample confirms these features despite a shift between the curves related to experimental uncertainties.

Figure 10 shows C/T vs T^2 plots restricted to the low-T range. The upper panel reports on the influence of the substitution content on the zero-field data, while the lower panel shows the influence of magnetic field in the case of $CaRu_{0.7}Ti_{0.3}O_3$. The data of $CaRuO_3$ in zero-field is consistent with the literature, showing a small upturn as T is decreased which leads to an extrapolation close to 80 mJ/K^2 mol for $T \rightarrow 0$.[5] The data of $CaRu_{1-x}Ti_xO_3$ are found to vary a lot with x, regarding both their shape and their location with respect to the "reference" curve of $CaRuO_3$. This evolution with x in $CaRu_{1-x}Ti_xO_3$ turns out to

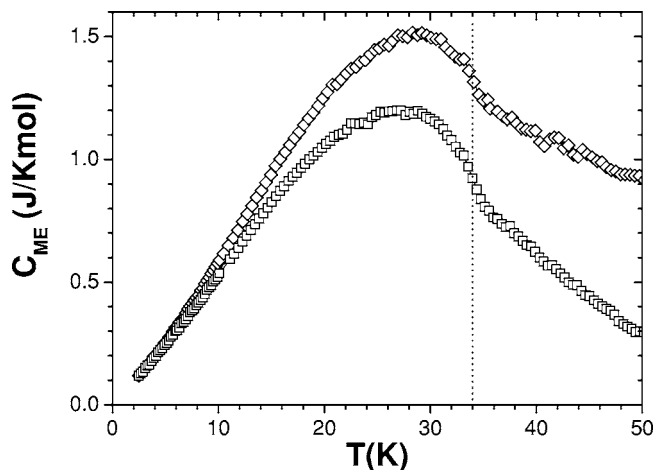FIG. 9. Temperature dependence of the (magnetic+electronic) contribution to heat capacity in two samples of $CaRu_{0.7}Ti_{0.3}O_3$ (see text about the procedure used to subtract the phononic term). The dashed line corresponds to $T_C = 34$ K derived from magnetic measurements.
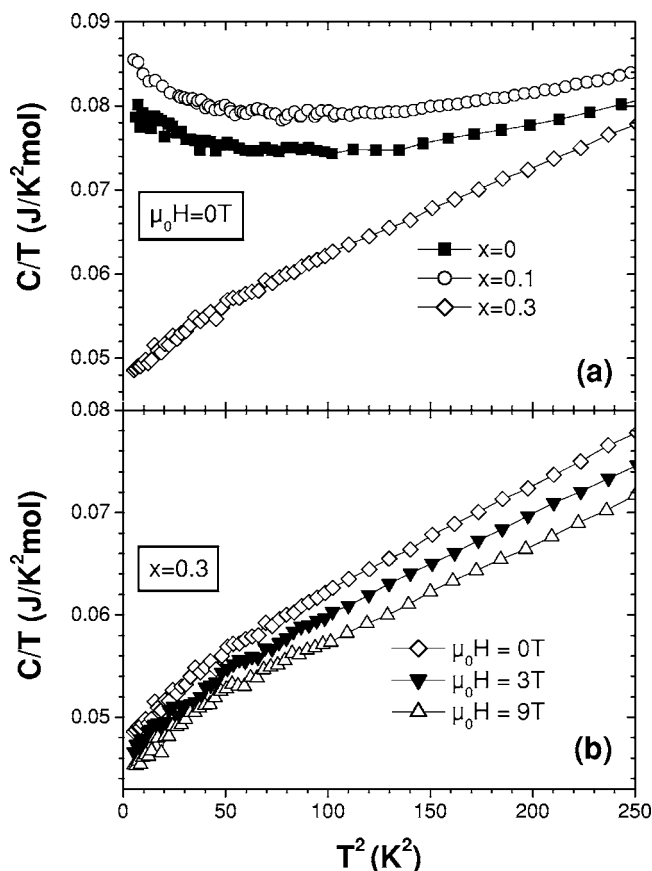
FIG. 10. Low-T heat capacity of $CaRu_{1-x}Ti_xO_3$ in C/T vs T^2 plots. Top panel: Influence of x on the zero-field data. Bottom panel: Influence of the magnetic field on the data for $x=0.3$.

be similar to the one observed by Kiyama et al.[5] as a function of y within the series $Ca_{1-y}Sr_yRuO_3$: for $y=0.2$, the C/T vs T^2 curve is located above the curve of $y=0$, while keeping the same upturn as $T \to 0$; whereas for $y=0.8$ (i.e., going further into the ferromagnetic side, as when increasing x up to 0.3 in our case), the C/T vs T^2 curve goes below that of $y=0$ and exhibits a slight downward curvature as $T \to 0$. Figure 10(b) shows that application of magnetic field leads to a progressive downward shift of the C/T vs T^2 curve of $CaRu_{0.7}Ti_{0.3}O_3$. Once again, we note that this behavior is similar to that observed for intermediate values of y within the series $Ca_{1-y}Sr_yRuO_3$.[5] As a matter of fact, application of 9 T in $Ca_{0.6}Sr_{0.4}RuO_3$ was found to reduce the low-T specific heat by about 10%, as is also roughly the case for $CaRu_{0.7}Ti_{0.3}O_3$. In their study of $Ca_{1-y}Sr_yRuO_3$, Kiyama et al.[5] showed that these specific heat features can be accounted for within the framework of the self-consistent renormalization model developed by Takahashi for nearly or weakly itinerant ferromagnets.[23]

IV. DISCUSSION

The problem of the origin of the substitution-induced ferromagnetism in $CaRu_{1-x}Ti_xO_3$ cannot be addressed without considering at the same time the question of the nature of this magnetism, i.e., localized or itinerant. The main experi-

mental features which must be accounted for in any interpretations are: (i) the large increase in ρ with x; (ii) the fact that the same value of T_C is found for all x values; (iii) the existence of a maximum in M_{rem} for $x=0.3$; (iv) the absence of a peak of heat capacity at T_C, accompanied by the presence of a rounded maximum below T_C.

A. Relevancy of localized magnetism to the experimental results

Let us first consider the case of localized ferromagnetism, since this type of magnetism is supposed to be favored by the introduction of disorder.[17,28] There are some experimental features tending to support localized magnetism:

(1) At first glance, the existence of a T_C independent of x is hardly compatible with itinerant magnetism, whereas it can be related to a characteristic spin-spin interaction in the case of localized magnetism.

(2) The persistence of the same T_C in compounds for which the resistivity is very large and exhibits a semiconductinglike behavior, i.e., transport features typical of localized magnetism [see for instance $x=0.8$ in Fig. 3(a)].

In this localized picture, one might speculate that the role of substitution by Ti ions is to break the electronic itinerancy, which in turn allows an underlying ferromagnetic interaction between localized Ru spins to be effective.

Let us now try to see whether the maximum in $M_{rem}(x)$ can be accounted for within such a framework. In a localized scenario, a maximum in M_{rem} means that the number of Ru ions participating in the ferromagnetic response exhibits a maximum for $x \sim 0.3$. Considering the random distribution between Ti and Ru, the question is thus to search for a type of local environment which can be expected to favor localized magnetism and which involves a maximum number of Ru when $x \sim 0.3$. The first idea is to consider some Ru clusters having a size small enough to differ from pure $CaRuO_3$. However, it must be emphasized that this maximum in M_{rem} occurs for a fraction of magnetic centers (Ru ions) that is ~ 0.7, i.e., well above the threshold for site percolation in a simple cubic lattice (~ 0.31). It was shown that there is no cluster of any size which shows a maximum within this filling range.[29] In this regime, almost all Ru ions are connected together and belong to the same *spanning big cluster*.[29] When investigating local environments different from clusters, one can consider that the basic requirements for a Ru to participate in the ferromagnetic response are just: (1) not to be surrounded only by other Ru (in order to generate a local situation different from that of $CaRuO_3$, since the latter is known to hinders ferromagnetism); (2) not to be surrounded only by Ti (in order to allow magnetic coupling with nearest-neighboring Ru). For a fraction $(1-x) \sim 0.7$, it turns out that such criteria correspond to the Ru ions that are located at the surface of the "big cluster." As schematically shown for two dimensions in the top of Fig. 11, this interface has an optimum for x lower than $x=1-x=0.5$ (this can be qualitatively ascribed to the fact that isolated Ru ions are excluded from this counting). Quantitatively, one can estimate the probability for a B site of $CaRuTiO_3$ to be an active Ru (i.e., a Ru
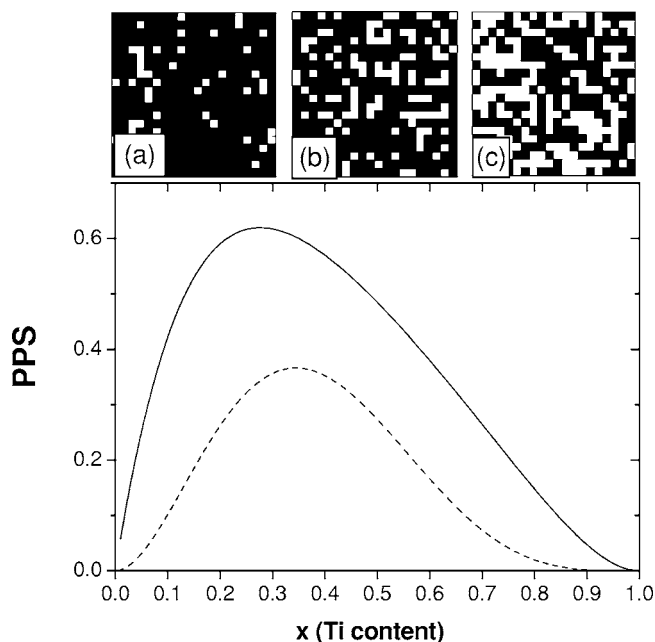
FIG. 11. Variation with x of the probability per site (PPS) to be a Ru having a number of Ru among its six nearest-neighbors, that is, in the range 1–5 (solid line) or in the range 3–4 (dashed line). The pictures at the top are simulations illustrating the random distribution of empty and filled "cells" on a 2D square lattice, x being the probability for a cell to be empty: (a) $x=0.1$; (b) $x=0.3$; (c) $x=0.5$.

meeting the above criteria) by using the binomial law. This probability per site (PPS) can be written as follows:

$$\text{PPS} = (1-x)\sum_{k=k_1}^{k_2} C_6^k (1-x)^k x^{(6-k)} \qquad (2)$$

with k being an integer in the range $0 < k < 6$. For the PPS to be a Ru at the surface of the big cluster, one must consider $k_1 = 1$ and $k_2 = 5$. This leads to the solid line in Fig. 11. One observes that this probability actually exhibits a maximum around $x \sim 0.3$, but its shape is more rounded than that of Fig. 6. Making the constraints more stringent (e.g., with $k_1 = 3$ and $k_2 = 4$), we note that one still obtains a maximum around $x \sim 0.3$ (dashed line) with a shape that is in better agreement with that of $M_{\text{rem}}(x)$. It must be emphasized, however, that this approach is clearly oversimplified and is not expected to provide us with a real fitting to the experimental $M_{\text{rem}}(x)$ curve. The point which deserves to be stressed is that the fraction of B-sites being Ru with Ti among their nearest-neighbors actually shows a maximum around $x \sim 0.3$.

We have discussed so far various issues which are favorable to—or at least consistent with—the localized nature of the substitution-induced FM. On the other hand, there are several main features which turn out to be hardly compatible with this assumption:

(a) Within the framework of localized magnetism, Ru^{4+} in a perovskite structure is supposed to be in a low-spin state ($S=1$), yielding a magnetic moment of $2\,\mu_B/\text{Ru}$. The maximum of M_{rem} for $x \sim 0.3$ is lower than $0.2\,\mu_B/\text{f.u.}$ (see Fig. 6), while the corresponding PPS is larger than 0.3 (see Fig. 11). This would mean that the maximum value of the magnetic moment per Ru taking part in the FM response is $\sim (0.2/0.3) \sim 0.66\,\mu_B/\text{Ru}$, a value not consistent with the expectation for Ru^{4+}.

(b) In the localized picture, the negative θ_{CW} values found for low x are not consistent with the existence of a FM transition.

(c) For localized magnetism, the height of the peak of heat capacity that is expected at T_C is of the order of $\Delta C = R[5S(S+1)]/[2S(S+1)+1]$, where S is the spin value and R the noble gas constant. With $S=1$ corresponding to Ru^{4+}, one thus expects $\Delta C = 2R$. To compare with the experimental curve that refers to a formula unit, one has to multiply ΔC by the PPS for a B-site to be an active Ru (i.e. a Ru participating in the FM ordering). Considering PPS at $x \sim 0.3$ in Fig. 11, one obtains values at least equal to ~ 6 J/K mol. Looking at Fig. 8, one can see that a peak of such a height should be clearly visible on the $C(T)$ curve. Therefore, the absence of this feature does not speak for a magnetism of localized nature.

Last but not least, the very mechanism that would be at the origin of the FM coupling is obscure. Firstly, the super-exchange between Ru^{4+} with large Ru-O-Ru angles (of the order of 150° in $CaRu_{1-x}Ti_xO_3$) is supposed to be antiferromagnetic. Secondly, a double-exchange mechanism leading to an effective FM coupling is not expected for Ru^{4+} because of the integer electron occupancy $(4d^4)$.[4]

Therefore, there are enough arguments against the relevancy of localized magnetism to justify a closer look at the possibility of itinerant magnetism.

B. Relevancy of itinerant magnetism to the experimental results

First, it must be underlined that a number of experimental results are typical of itinerant magnetism:

(1) The values of θ_{CW} that can be <0 or >0;

(2) The location of the data on the generalized Rhodes-Wohlfarth plot;

(3) The heat capacity features: The existence of a bump below T_C on the C/T vs T^2 plot, as well as a kink at T_C on the $C_{\text{ME}}(T)$ plot are signatures found in typical weakly itinerant ferromagnets like Sc_3In.[30] Moreover, the influence of the magnetic field on the low-T heat capacity is very similar to that encountered for $ZrZn_2$ which is another well known weakly itinerant ferromagnet.[30] Finally, we also noticed the similarity of our $C(T)$ data with that of the $Ca_{1-y}Sr_yRuO_3$ series, a system where the evolution of the properties with y can be described within the framework of itinerant ferromagnetism.[5]

A basic issue is to see how the appearance of FM can be accounted for within such a framework. When substituting Ru^{4+} by Ti^{4+}, there are two main effects from the viewpoint of band magnetism: 1. the size mismatch can modify the structural distortions and thus change the bandwidth; 2. replacement of Ru^{4+} $(4d^4)$ by Ti^{4+} $(3d^0)$ directly affects the band filling.

Let us try to compare the impact of these two phenomena. In $CaRu_{1-x}Ti_xO_3$, the cationic radius of Ti^{4+} (0.0605 nm) is just a bit smaller than that of Ru^{4+} (0.0620 nm). We note that this variation in radius is about one order of magnitude smaller than when substituting Ca^{2+} (0.134 nm) by Sr^{2+} (0.144 nm) on the A site. The amplitude of the distortions is linked to the value of the tolerance factor $t=(r_A+r_O)/\sqrt{2}(r_B+r_O)$, where r_A, r_B, and r_O are the ionic radii for the A-site, B-site, and oxygen, respectively. The r_B of Ti^{4+} and Ru^{4+} being very close to each other, this substitution is not expected to produce large changes in the structural distortions. It is worth noticing that t of $CaRu_{1-x}Ti_xO_3$ for $x=0.3$ is about the same as the one for $y=0.05$ in $Ca_{1-y}Sr_yRuO_3$, while ferromagnetism only appears for $y > 0.2$ in this latter system.[3] Another indication of the weak impact of the size effect in our data comes from the results obtained with Zr substitution. While Zr^{4+} has a cationic radius (0.072 nm) *larger* than that of Ru^{4+}, it was found to generate FM just like Ti^{4+} which has a radius *smaller* than that of Ru^{4+}. In other respects, the decrease of the band filling resulting from the substitution of Ru^{4+} ($4d^4$) by Ti^{4+} ($3d^0$) or Zr^{4+} ($4d^0$) is expected to have a significant impact that should be of identical importance in both cases. Considering $CaRu_{1-x}Ti_xO_3$, the variation in the density n of $4d$ electrons is $\Delta n \sim -xn$. For small x values, one can use as a first approximation a rigid-band picture, for which the main features of the spectrum of density of states (DOS) are supposed not to be affected by the band filling. Within such an assumption, increasing x leads to shift the Fermi energy E_F towards the lower energy side of the DOS curve. Inspecting the DOS of $CaRuO_3$ reported in the literature,[4,31] one observes the presence of sharp peaks located at energies slightly lower than $E_F(x=0)$. Therefore, there must be a range of x values for which $N[E_F(x)]$ is significantly larger than $N[E_F(x=0)]$. Within the band-structure-based Stoner theory, itinerant ferromagnetism takes place when $N(E_F)I > 1$, I being the Stoner parameter. In $CaRuO_3$—which is known to be on the verge of FM—it has been found from NMR data[7] that $N(E_F)I \sim 0.98$. One can thus expect that a small increase in $N(E_F)$ can easily make the Stoner criterion to be fulfilled and trigger the setting of ferromagnetic order. It is worth noting that the same type of interpretation was proposed to account for the appearance of FM in various systems, such as $AlFe_{1-x}Mn_x$ (Ref. 32) or $La_{1-x}Sr_xCoO_3$.[33] On the other hand, it must also be emphasized that this scenario is clearly oversimplified and, in our case, it can only hold for x values that are not too large. As it was detailed on the basis of conductivity measurements in the case of $SrRu_{1-x}Ti_xO_3$, the combination of disorder and electron correlation effects must produce strong modifications of the DOS curve for large x values.[34] Investigating the evolution of DOS with x, Kim et al.[34] suggested first a suppression of the peak near E_F (for $x \sim 0.3$), followed by the opening of a gap (for $x \sim 0.5$) which progressively widens to eventually lead to the diamagnetic insulating behavior of $CaTiO_3$ ($x=1$).

Obviously, the simple mechanism described above within a rigid-band approximation cannot justify the persistence of FM with the same T_C for all x values. It appears that the only way to reconcile this observation with the above itinerant

picture is to consider that $CaRu_{1-x}Ti_xO_3$ is *magnetically heterogeneous*, i.e., a system in which a short-range FM develops only for a certain range of local Ti content, with a maximum T_C of 34 K. As it will be discussed below, it turns out that the few requirements on which relies such an assumption are likely to be fulfilled in the case of $CaRu_{1-x}Ti_xO_3$. It must also be emphasized that He et al.[14] were previously led to introduce this concept of heterogeneous ferromagnetism in their investigation of $CaRu_{1-x}M_xO_3$ with magnetic ions such as M=Fe, Ni, and Mn. The requirements for the above described heterogeneity in $CaRu_{1-x}Ti_xO_3$ are:

1. The random distribution between Ru and Ti leads to a wide range of local x_{loc} for any given value of the average content, hereafter referred to as x_{av}. Whatever x_{av}, one can find regions characterized by x_{loc} values very different from x_{av}, especially if considering regions that are small enough. It can even be anticipated that the shorter is the length scale considered, the wider is the effective distribution of x_{loc}.

2. Physical properties of ruthenates are sensitive to the local environment, from both chemical and structural viewpoints. As a result, a property measured on a sample of a given average composition can be regarded as the superimposition of short-scale responses corresponding to a variety of local compositions.

3. The Ti-induced FM in $CaRu_{1-x}Ti_xO_3$ takes place within a limited range of x_{loc}, and it exhibits a maximum of $T_C (x_{loc})$ that is equal to 34 K.

Within such a framework, one can consider that, for all x_{av} values, there are regions where x_{loc} yields the optimal T_C, which leads us to always observe the same $T_C=34$ K in our magnetic measurements. Moreover, one can also consider that the optimum of FM signal found for $x_{av} \sim 0.3$ simply derives from the fact that the range of x_{loc} leading to FM is centered at $x_{loc} \sim 0.3$. Finally, we note that the evolution of $\rho(T)$ with x_{av} towards an insulating behavior is not inconsistent with the existence of short-range itinerant FM, provided that the volume fraction occupied by these regions is lower than the percolation threshold.

Let us now address the relevancy to $CaRu_{1-x}Ti_xO_3$ of each of the three above issues. First, it can be noted that the existence of a dilution-induced itinerant FM was previously reported in $Y(Co_{1-x}Al_x)_2$ for a given range of $x(0.13 \leq x \leq 0.19)$.[35] The Curie temperature and the spontaneous magnetic moment display maximum values close to the midpoint of this range ($x \sim 0.15$). The appearance of FM in $Y(Co_{1-x}Al_x)_2$ was discussed in terms of a crossover from nearly ferromagnetic to a weakly ferromagnetic phase.[35] Secondly, several experimental results have pointed to a great sensitivity of the ruthenates to the local environment. For instance, in their study of $SrRu_{1-v}O_3$ compounds, Dabrowski et al. invoked the possibility of a crucial role of local disorder.[36] Similarly, in their comparison of the isoelectronic $Sr_x(Na_{0.5}La_{0.5})_{1-x}RuO_3$ and $Sr_xCa_{1-x}RuO_3$ series, He et al.[12] observed a faster suppression of the long-range FM in the former case, a feature they attributed to an effect of charge disorder on the A sites which affects the local environment of Ru atoms. Finally, one can also note that Miéville et al.[37] showed that the reduction of remanent magnetization versus x in $SrRu_{1-x}Ti_xO_3$ can be accounted for in a local picture,

considering only the neighboring configurations of a B site.

Let us address in more details the third issue mentioned above, namely the length-scale dependence of the effective distribution of x_{loc}. We emphasize that the distribution considered here is basically different from local fluctuations in composition due to imperfections in the synthesis procedure, as it is often encountered with standard solid-state reaction. Our EDS investigations actually demonstrated this latter type of inhomogeneity in our $CaRu_{1-x}Ti_xO_3$ samples. However, the data also indicates that this "grain to grain" inhomogeneity is not large enough to account for the evolution of the physical properties. For instance, the lowest Ti content found in the EDS investigations of $x_{av}=0.7$ is about 0.45 [see inset (b) of Fig. 1], which cannot account for the sizeable value of $M_{rem}(x_{av}=0.7)$ (see Fig. 6), if this remanent magnetization is linked to local contents close to 0.3 as it is assumed in our picture. It must be noted that these EDS analyses were carried out with an electron beam size such that they reflect the mean composition over a region of typical volume l^3, with l in the range $10-100$ nm. As discussed above, the characteristic length scale relevant to the physical properties in $CaRu_{1-x}Ti_xO_3$ is probably smaller.

In what follows, we thus consider a well defined x_{av} (identical throughout the whole sample) and we focus on the distribution of x_{loc} that merely results from the random nature of the substitution. The statistics is still governed by the binomial law as previously used in Eq. (2), but now one must not only consider the six nearest-neighbors of each magnetic centers (Ru ions). For a given x_{av}, the point is to estimate the local content x_{loc} averaged over a characteristic volume whose size corresponds to a certain number of B sites.

Let us recall the binomial law in a form relevant to the present situation: If p is the probability for a B site to be occupied by a Ti ion $[(1-p)$ for a Ru ion], the probability to actually find k Ti when considering a set of n sites is

$$P(n,k,p) = C_n^k p^k (1-p)^{n-k} \text{ with } \sum_{k=0}^{n} P(n,k,p) = 1. \quad (3)$$

The question we raised can thus be formulated as follows: For a given p (i.e., x_{av}), what is the evolution of the distribution of local Ti content (i.e. $k/n=x_{loc}$) as a function of the size of domains considered (i.e., n)?

This distribution of x_{loc} is given by the probability

$$P(n,x_{loc},x_{av}) = C_n^{nx_{loc}} x_{av}^{nx_{loc}} (1-x_{av})^{n(1-x_{loc})} \quad (4)$$

with

$$\sum_{x_{loc}=0}^{1} P(n,x_{loc},x_{av}) = 1.$$

This probability can only be calculated for x_{loc} values such that nx_{loc} is an integer, i.e., $(n+1)$ points between 0 and 1, separated by $\Delta x_{loc}=1/n$. Therefore, to make comparable the probabilities calculated for different n values, one has to consider the differential probability
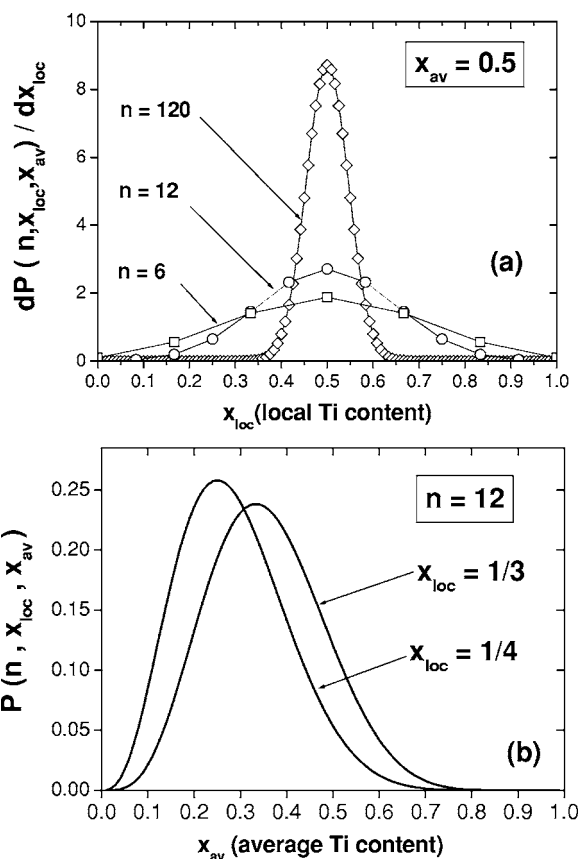

FIG. 12. Calculation of the probabilities to find a local Ti content of x_{loc} when considering n B sites, the average Ti content being x_{av} in $CaRu_{1-x_{av}}Ti_{x_{av}}O_3$ (see text for details). Top panel: Influence of n on the distribution of x_{loc} for a given $x_{av}(=0.5)$. Bottom panel: Variation with x_{av} of the probability to find a local content x_{loc} around 0.3 (e.g., in between 1/4 and 1/3), for an elemental volume corresponding to 12 B sites of the perovskite structure.

$$\frac{dP(n,x_{loc},x_{av})}{dx_{loc}} = nP(n,x_{loc},x_{av}), \quad (5)$$

so that

$$\int_0^1 \frac{dP(n,x_{loc},x_{av})}{dx_{loc}} dx_{loc} \simeq \sum_{x_{loc}=0}^{1} nP(n,x_{loc},x_{av})\Delta x_{loc} = 1.$$

Figure 12(a) illustrates the influence of n on the distribution of x_{loc} in the case $x_{av}=0.5$. One observes that the distribution is progressively broadened as n is decreased.[38] In the case $n=6$, the probability to find x_{loc} equal to 0.25 or 0.75 is just half that corresponding to $x_{loc}=x_{av}=0.5$. Ascribing the Ti-induced FM to regions characterized by x_{loc} within a certain range around 0.3, one can try to estimate which typical size of domains (i.e., n value) could account for the variation of $M_{rem}(x_{av})$ shown in Fig. 6. We assume here that $M_{rem}(\mu_B/\text{f.u.})$ is proportional to the volume fraction of the sample where x_{loc} is roughly in between 1/4 and 1/3. As shown in Fig. 12(b), we found that values of n close to 12 lead to profiles that are in reasonable agreement with the shape of Fig. 6.[39] The curves of Fig. 12(b) also allow us to

estimate the volume fraction involved in the FM response. For instance with $x_{av}=0.3$, this fraction is ~ 0.23 for both 1/4 and 1/3, leading to ~ 0.46. Taking this into account, the actual p_S changes from 0.23 μ_B/Ru to $0.35(=0.23\times 0.7/0.46)\mu_B$/Ru, when considering only the active Ru ions. It can be checked that, even with this correction, one still has $p_{eff}/p_S \gg 1$, as expected for itinerant ferromagnetism. It can also be noted that the p_S characteristic of FM in $CaRu_{1-x}Ti_xO_3$ (~ 0.35 μ_B/active Ru with $T_C \sim 34$ K) is lower than but of same order of magnitude as the value found in the related itinerant ferromagnet $SrRuO_3$ (~ 1.4 μ_B/Ru with $T_C \sim 165$ K).[3]

V. CONCLUSION

The ferromagnetism (FM) induced by Ti substitution on the B site of $CaRuO_3$ has been investigated by means of magnetization, resistivity and heat capacity measurements. This study was carried out for $0.1 \leqslant x \leqslant 0.9$ within the series $CaRu_{1-x}Ti_xO_3$. The most salient experimental features to be noted are (i) a large, systematic increase in ρ with x; (ii) the observation of the same value of T_C for all x values; (iii) the existence of a maximum in M_{rem} for $x=0.3$; (iv) no peak of heat capacity at T_C, while there is a rounded maximum below T_C. It must be noted that the first three issues are in good overall agreement with the previous studies performed by He *et al.*[13] and Felner *et al.*[16]

The possible origins of this ferromagnetism have been discussed along with the question of its nature, namely, localized or itinerant. It appears that important features can hardly be accounted for in the framework of localized magnetism. Actually, the mechanism found to be the most consistent with the whole set of data can be summarized as follows: $CaRu_{1-x}Ti_xO_3$ is a magnetically heterogeneous system; it presents short-range ferromagnetism, associated with regions where the value of the local Ti content is within a certain interval centered at $x_{loc} \sim 0.3$. The maximum of $T_C(x_{loc})$ is 34 K; this ferromagnetism is basically of itinerant nature; its appearance would result from a nearly to weakly itinerant FM crossover driven by reduction in the band filling.

Though some aspects of this picture remain speculative so far, it should be underlined that—beyond the details of the mechanism—the data clearly points to the short-range nature of this induced FM, a feature which implies that the statistics of the random distribution must play a crucial role.

More work has to be performed on $CaRu_{1-x}Ti_xO_3$ to test the reliability of the picture described above. For instance, it is clear that local investigations of the magnetism by complementary techniques such as nuclear magnetic resonance would be highly desirable. Besides, direct band-structure calculations in clusters representative of $CaRu_{1-x}Ti_xO_3$ should be performed.

[1] Y. Maeno, H. Hashimoto, K. Yoshida, S. Nishizaki, T. Fujita, J. G. Bednorz, and F. Lichtenberg, Nature (London) **372**, 532 (1994).

[2] G. Cao, S. McCall, J. Bolivar, M. Shepard, F. Freibert, P. Henning, J. E. Crow, and T. Yuen, Phys. Rev. B **54**, 15144 (1996).

[3] G. Cao, S. McCall, M. Shepard, J. E. Crow, and R. P. Guertin, Phys. Rev. B **56**, 321 (1997).

[4] I. I. Mazin and D. J. Singh, Phys. Rev. B **56**, 2556 (1997).

[5] T. Kiyama, K. Yoshimura, K. Kosuge, H. Michor, and G. Hilscher, J. Phys. Soc. Jpn. **67**, 307 (1998).

[6] K. Yoshimura, T. Imai, T. Kiyama, K. R. Thurber, A. W. Hunt, and K. Kosuge, Phys. Rev. Lett. **83**, 4397 (1999).

[7] H. Mukuda, K. Ishida, Y. Kitaoka, K. Asayama, R. Kanno, and M. Takano, Phys. Rev. B **60**, 12279 (1999).

[8] J. J. Randall and R. Ward, J. Am. Chem. Soc. **81**, 2629 (1959).

[9] J. M. Longo, P. M. Raccah, and J. B. Goodenough, J. Appl. Phys. **39**, 1327 (1968).

[10] T. C. Gibb, R. G. Greatex, N. N. Greenwood, and P. Kaspi, J. Chem. Soc. Dalton Trans. **12**, 1253 (1973).

[11] I. Felner, I. Nowik, I. Bradaric, and M. Gospodinov, Phys. Rev. B **62**, 11332 (2000).

[12] T. He, Q. Huang, and R. J. Cava, Phys. Rev. B **63**, 024402 (2000).

[13] T. He and R. J. Cava, Phys. Rev. B **63**, 172403 (2001).

[14] T. He and R. J. Cava, J. Phys.: Condens. Matter **13**, 8347 (2001).

[15] A. Maignan, C. Martin, M. Hervieu, and B. Raveau, Solid State Commun. **117**, 377 (2001).

[16] I. Felner, U. Asaf, I. Nowik, and I. Bradaric, Phys. Rev. B **66**, 054418 (2002).

[17] G. Cao, F. Freibert, and J. E. Crow, J. Appl. Phys. **81**, 3884 (1997).

[18] I. M. Bradaric, I. Felner, and M. Gospodinov, Phys. Rev. B **65**, 024421 (2001).

[19] J. Rodriguez-Carvajal, LLB (2005).

[20] G. Cao, C. S. Alexander, S. McCall, J. E. Crow, and R. P. Guertin, Mater. Sci. Eng., B **63**, 76 (1999).

[21] In Ref. 13, an optimum in $M_{rem}(x)$ was also reported, but the maximum was a bit lower ~ 0.06 μ_B/f.u., and it was observed at $x \sim 0.4$.

[22] T. Moriya, J. Magn. Magn. Mater. **14**, 1 (1979).

[23] Y. Takahashi, J. Phys. Soc. Jpn. **55**, 3553 (1986).

[24] A. L. Dawson, D. H. Ryan, and D. V. Baxter, Phys. Rev. B **54**, 12238 (1996).

[25] P. R. Rhodes and E. P. Wohlfarth, Proc. R. Soc. London, Ser. A **273**, 247 (1963).

[26] M. Bouvier, P. Lethuillier, and D. Schmitt, Phys. Rev. B **43**, 13137 (1991).

[27] S. Ikeda, Y. Maeno, and T. Fujita, Phys. Rev. B **57**, 978 (1998).

[28] D. A. Crandles, M. Reedyk, R. W. Schaeffer, A. E. Hultgren, and R. Schlee, Phys. Rev. B **65**, 224407 (2002).

[29] J. M. D. Coey, Phys. Rev. B **6**, 3240 (1972).

[30] K. Ikeda, S. K. Dhar, M. Yoshizawa, and K. A. Gschneidner, J.

Magn. Magn. Mater. **100**, 292 (1991).

[31] P. Ravindran, R. Vidya, P. Vajeeston, A. Kjekshus, H. Fjellvag, and B. C. Hauback, Solid State Commun. **124**, 293 (2002).

[32] D. A. Papaconstantopoulos, I. I. Mazin, and K. B. Hathaway, J. Appl. Phys. **89**, 6889 (2001).

[33] P. Ravindran, P. A. Korzhavyi, H. Fjellvag, and A. Kjekshus, Phys. Rev. B **60**, 16423 (1999).

[34] K. W. Kim, J. S. Lee, T. W. Noh, S. R. Lee, and K. Char, Phys. Rev. B **71**, 125104 (2005).

[35] K. Yoshimura, M. Mekata, M. Takigawa, Y. Takahashi, and H. Yasuoka, Phys. Rev. B **37**, 3593 (1988).

[36] B. Dabrowski, O. Chmaissem, P. W. Klamut, S. Kolesnik, M. Maxwell, J. Mais, Y. Ito, B. D. Armstrong, J. D. Jorgensen, and S. Short, Phys. Rev. B **70**, 014423 (2004).

[37] L. Miéville, T. H. Geballe, L. Antognazza, and K. Char, Appl. Phys. Lett. **70**, 126 (1997).

[38] Even though it can only be calculated for a series of values, the distribution of x_{loc} is basically continuous.

[39] The agreement is, however, far from being perfect, as it is well visible on the high-x_{av} side of Fig. 12(b), where the calculated curves vanish faster than M_{rem} in Fig. 6. Note that a better agreement could likely be obtained by also taking into account the existence of a "grain to grain" variation in average composition, as displayed in the insets of Fig. 1.